Available online at www.sciencedirect.com

ScienceDirect

Physics Procedia 56 (2014) 875 – 884

Physics Procedia

8th International Conference on Photonic Technologies LANE 2014

Experimental comparison of laser cutting of steel with fiber and CO_2 lasers on the basis of minimal roughness

A.M. Orishich[a], A.G. Malikov[a], V.B. Shulyatyev[a,*] , A.A. Golyshev[a]

[a]*Khristianovich Institute of Theoretical and Applied Mechanics, SB RAS, Institutskaja 4/1, 630090 Novosibirsk, Russia*

Abstract

The fiber and CO_2 laser were compared from the viewpoint of two laser-cutting methods: the oxygen-assisted cutting of low-carbon steel and fusion cutting of stainless steel with a neutral assistant gas. The absorbed laser energy was measured in respect to the unit of the removed material volume at the cutting parameters correlating to the minimal roughness of the cut surface. This value equals to 11…13 J/mm^3 both for the fiber and CO_2 lasers. During the fiber-laser cutting, the minimal roughness is reached at the Peclet number 0.35…0.4, at the CO_2-laser cutting – at 0.45…0.55. At the fusion cutting of stainless steel, the minimal roughness is reached at the maximal cutting speed. The maximal cutting speed has the higher value in the fiber-laser case at the same laser power. The paper discusses the potentiality of the method of absorbed laser energy measurement by the value difference at the cut channel inlet and outlet.

Peer-review under responsibility of the Bayerisches Laserzentrum GmbH

Keywords: fiber laser; CO_2 laser; cutting; roughness; beam absorption

Nomenclature

W	laser power
V	cutting speed
t	sheet thickness

* Corresponding author. Tel.: +7-3833307856; fax: +7-3833307342 .
E-mail address: shulyat@rambler.ru

Peer-review under responsibility of the Bayerisches Laserzentrum GmbH
doi:10.1016/j.phpro.2014.08.106

b	kerf width
λ	laser wave length
k	thermal conductivity
a	thermal diffusivity
T_m	melting temperature

1. Introduction

Today, two types of lasers are in use for metal cutting, namely the CO_2 and fiber lasers. Each type has its advantages and disadvantages. The CO_2 laser is able to cut metals within the wide range of thicknesses, with the good quality. The fiber laser is more compact, has better performance characteristics and permits cutting thin (up to 4 mm) sheets with higher speed [1]. However, when cutting thick sheets, the fiber laser ranks below the CO_2 laser in quality at the comparable cutting speed. The quality means, above all, low cut surface roughness. The seek for the physical reasons of this difference and ways of increase of thick sheets cutting quality by the fiber laser is now one of the leading directions in the investigation of the laser cutting of metals.

At the moment, most researchers accept that the fundamental base of the different cut quality by the fiber and CO_2 laser (in the case of thick sheets) is different dependence of the laser-radiation absorption coefficient at the cut front on the angle of incidence and different properties of focused beams [2]. Experts present various hypotheses about the direct physical origins of the different cut quality in the cases of the fiber and CO_2 lasers, and the conclusions result from the comparison of the cutting by the fiber and CO_2 lasers [3-5]. The direct experimental comparison of the fiber- and CO_2 cutting is carried out for the better understanding of both processes peculiarities.

In the present work, the cuttings by the fiber and CO_2 laser are compared experimentally under the condition of the minimal roughness of the cut surface. Under study was the oxygen-assisted laser cutting of low-carbon steel, and the fusion cutting of stainless steel. In [6-7], we showed that at the process of the oxygen-assisted laser cutting of low-carbon steel within the wide range of sheet thickness, the minimal cut-surface roughness is reached at a certain value of the laser energy input into a unit of the material volume removed from the cut channel. In [6-7], the CO_2 laser was used for the cutting. In the present work, the absorption coefficient of the fiber laser beam was measured during the cutting; the laser energy consumed for the cut with the minimal surface roughness was found; the obtained data were compared with the CO_2 laser.

2. Experimental procedure

The ytterbium laser IPG/IRE-Polus was used; its power was 2 kW, the collimator was IPG, model D5-WC/AC. The beam parameter product (BPP, the product of the beam radius in the near zone by the angular beam radius in the far zone) was equal to 3.8 mm·mrad. The beam diameter in the focusing lens after the collimator was 17 mm, the lens focal distance was 200 mm. Low-carbon steel sheets of 3, 5, and 10 mm were cut at the radiation power from 0.5 to 2 kW. The continuous CO_2 laser was also used; its BPP was 4.7 mm·mrad [8]. The cutting was done by the circular-polarization radiation by the conventional scheme, the radiation power ranged from 0.5 to 3.5 kW. The radiation was focused by the ZnSe lens with the focal distance of 190 mm. The beam diameter on the lens was equal to 25 mm. The diameter of the focused beam in its waist was evaluated as a sum of the diffraction diameter and diameter of the dissipation spot resulting from the spherical aberration. The calculated total diameter is 180 μm for the fiber laser and 200 μm for the CO_2 laser.

The fiber laser cut the sheets of 3, 5, and 10 mm, the CO_2 laser – of 5, 10, and 16 mm. The oxygen jet was formed by a conic nozzle at the excessive gas pressure in the laser cutter chamber of 0.25 MPa as the sheets of 3 mm were cut, and of 0.05 MPa at all other thicknesses.

The value of surface roughness (characteristic height of nonuniformities) measured with a laser confocal scanning microscope Olympus LEXT in two cross sections (near the upper and near the lower sheet surfaces) was adopted as a quality criterion. For this sample, the biggest from two values was taken to be characteristic one.

Absorption coefficient A is found on the method [4, 9] from the relation:

$$A = \frac{W - W_{tr}}{W},$$

where W is the laser power before the focusing lens, W_{tr} is the laser power passed through the cut channel durring the process. Here, the absorption coefficient means the integral coefficient which includes also the laser power absorbed at multiple reflections in the cut channel. The measurement process is schematically shown in Fig. 1.

The power meter was installed on a bracket which is mechanically connected to a cutting head and moves together with it during the cutting process. In the experiment, the power meter OPHIR 5000W-CAL-SH was used. The position of the receiving area of the meter provided that all passed radiation hit onto the meter. Destruction products, metal and oxide drops were blown away with the transversal flow of air, and they could not reach the receiver.

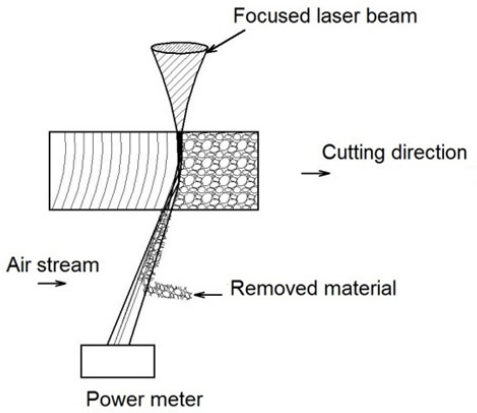

Fig. 1. Schematic of the absorbtion coefficient measurement.

3. Experimental results

3.1. Oxygen-assisted laser cutting

Square samples were cut out from the sheets of low-carbon steel St3 (clone of St37-2). The sheets of 3, 5, 10 and 16 mm were cut at the laser power ranging from 0.5 to 2 kW with fiber laser and 0.5 to 3.5 kW with CO_2 laser. The oxygen pressure in the laser head chamber was chosen in such a manner to provide the minimal roughness of the cut surface. Oxygen pressure in the laser head was 2.5 bar as the sheet thickness was 3 mm, 0.5 bar at other thickness, the gas-dynamic nozzle diameter is 1.5 mm at any thickness.

During the experiments, under study was the dependence of the cutting surface roughness on the cutting speed, focused beam waist position about the sheet surface, and laser power. The optimum values of these parameters at which the roughness was minimal, were to be found. The optimal parameters were found in two stages. First, optimization was done by two parameters: for the assigned power value, the optimal position of the waist and cutting speed were found, the cutting speed is then refereed to as V^*. The cut width depended on the focus position; the optimal value of the width b^* was determined for each power. Then, at the second stage, the optimization was done by the laser power. From the couples V^* and b^*, corresponding to different power levels, those were chosen at which the cut surface roughness was minimal. These values are designated as V_{opt} and b_{opt}, and the respective laser power was accepted as the optimal one.

The maximum data volume was obtained for the thickness of 5 mm. For a number of power values, the dependence of the roughness on the cutting speed was registered. Fig. 2 shows the photos of the cut surface as the power was 1 kW, at optimum cutting parameters, corresponding to minimal roughness.

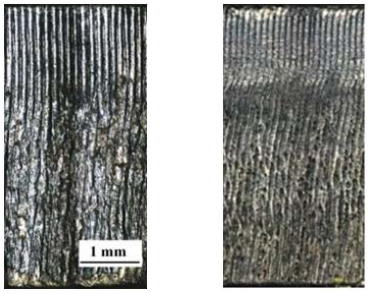

a B

Fig. 2. Photo of the cut surface at the optimal cutting parameters correlating with the minimal roughness, t = 5 mm. (a) fiber laser; (b) CO_2 laser.

Note the similarity of the surface morphologies. Both photos show two zones – one with even striations near the top edge of the sheet, and the other with more chaotic ones in the bottom part. The ratio of zones depth, striation pitch, and inclination angle are similar for both laser types.

Fig. 3 presents the generalized result of optimization for two laser types, and for different sheet thicknesses. The results are presented as the Peclet number $Pe^* = V^*b^*/a$ (dimensionless speed) versus the relative dimensionless power $Q = W/ktT_m$. Thermophysical characteristics were accepted for pure iron.

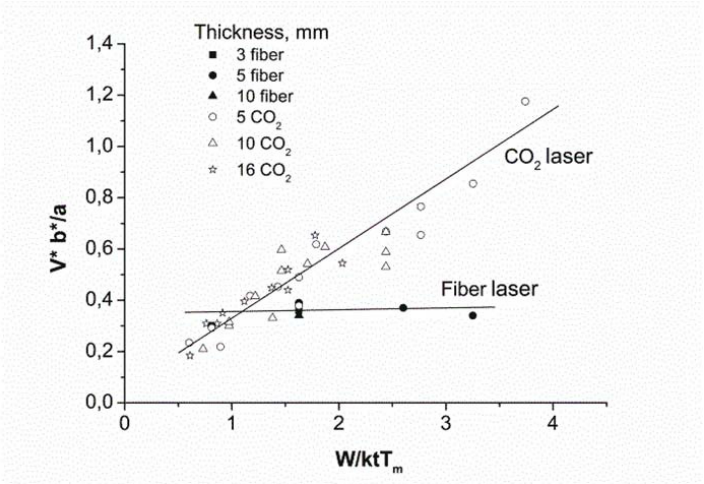

Fig. 3. Peclet number Pe^* optimiuzed by the cutting speed and cut width versus relative dimensionless power.

The points presented in Fig. 3 were obtained as follows. For the different sheet thicknesses and laser power levels, the dependence of the roughness R_a on cutting speed V and on cut width b (position of the focused beam waist about the sheet surface) was measured. The values of V^* and b^* were found at which the roughness was minimal. The second condition was the absence of dross. The optimal value of the speed V^* was always lower than its maximal value, i.e. at the assigned t and W, the minimum of the dependence $R_a(V)$ was observed.

As is seen from Fig. 3, in the dimensionless coordinates, the data for various thicknesses are described with the same dependence, and its view depends on the laser type. In the case of the fiber laser, the dependence of the Peclet number optimized by two parameters, on the power is “degenerate”, i.e. different values of the laser power correlate with the same (within experimental error limits) optimal value of the Peclet number. Thus, within the studied parameters range, during the fiber-laser cutting, in order to reach the minimal roughness optimized by the cutting speed and cut width (focus position), it is necessary to provide the Peclet number $Pe_{opt} = V_{opt}b_{opt}/a = 0.35$ regardless the cut sheet thickness and laser power.

In the case of CO_2 laser, different values of the dimensionless power correspond to the different optimal Peclet

numbers, and the dependence $Pe^*(W/ktT_m)$ approaches to the linear one. The measurements show that the roughness correlating with the optimal cutting speed and cut width depends on the power – it is measured along the lines presented in Fig. 3 of the dependence $Pe^*(W/ktT_m)$. The roughness minimum is reached at Q = 1.6, which corresponds to $Pe_{opt} = 0.5$.

The value $E = W/Vtb$ is the laser energy applied to the unit of the material volume removed from the cut channel. The ratio Q/Pe^* presents the same value in the dimensionless form. As is seen from Fig. 3, in the case of CO_2 laser, E is the same within the whole range of values W/t, and in the case of the fiber laser, different W/t correlate with different E.

The generalized variable W/ktT_m contains the laser power W before the focusing lens. But absorbed energy is the component of the energy balance of the laser cutting. The absorption coefficient of the laser power was measured during the laser cutting in order to study deeper the energy conditions of the laser cutting. The dependdence of absorption coefficient on the cutting speed was measured at different values of the radiatioon power. The focused-beam waist position corresponded to the roughness minimum.

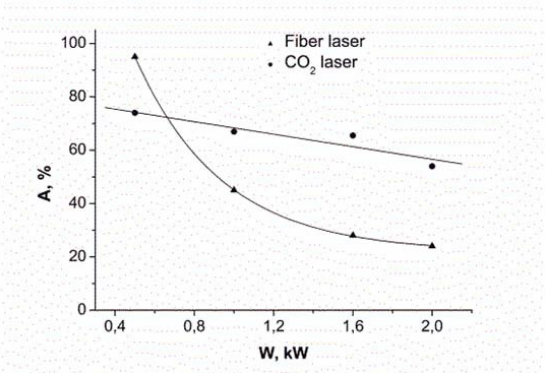

Fig. 4. Absorption coefficient of the laser power in the cut channel versus incident power at the optimal cutting speed.

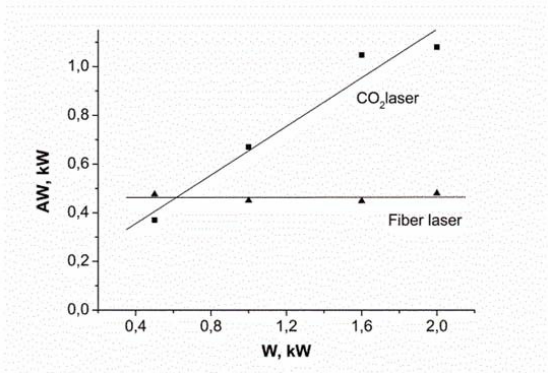

Fig. 5. The laser power absorbed in the cut channel vesrus the incident power at the optimal cutting speed.

Fig. 4 shows the absorption coefficient of the laser power in the cut channel versus incident power at the optimal cutting speed which corresponds to the minimal roughness. Evident that as the power rises, the absorption coefficient decreases significantly in the fiber-laser case. Withih the power range of 0.5…2 kW, it decreases from 95 to 25 %. In the CO_2 laser case, it decreases too but weaker: from 75 to 55 %. As a result, the power absorbed in the channel (Fig. 5) rises in the CO_2 laser case and remains constant in the fiber-laser case. Note the similar type of dependences in Fig. 3 and Fig. 5.

In the fiber-laser case, the measured absorption coefficient is 0.95. It is much higher than the maximum value of about 0.5 calculated by the Fresnel formulas for the iron melt and flat surface at a single reflection [2]. This exceeding may result from the difference between the absorption conditions in the laser-cut channel and idealized ones in [2]. The real surface of the cut front may deviate significantly from the flat shape, with various inhomogeneities due to instabilities in the melt flow [5]. Because of this, the laser beam propagation pattern may be complex, with multiple reflections from the cut front and side channel walls. As the reflection quantity rises, the absorption coefficient increases too. Multiple reflections in the narrow channel can occur even without instabilities. Moreover, the cut channel surface is covered with a oxide film which may also cause the increase of the absorption coefficient in respect to pure iron.

If the absorbed power is used as the dimensionless laser power for the expression of the experimental data corresponding to the minimal roughness (Fig. 6), the experimental dependence $Pe^*(AW/ktT_m)$ does not change significantly in the CO_2 laser case, it remains almost linear, and just its inclination changes. At the same time, the dependence for the fiber laser changes dramatically – all data are focused in one spot, and this spot lies on the line corresponding to the CO_2 laser. It means that AW/Vtb is the same for the two laser types. This is a fundamental result: both for the CO_2 and fiber laser, the minimal roughness of the cut surface is reached at the same absorbed laser energy applied to the volume unit of the material removed from the cut channel. This value is 11…13 J/mm^3.

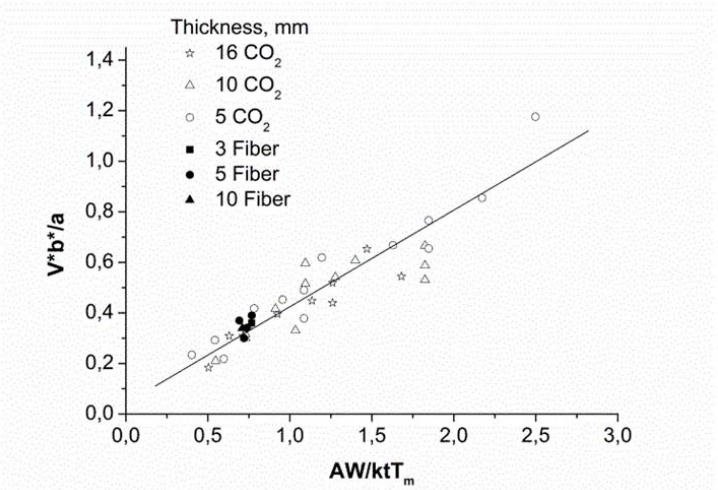

Fig. 6. Peclet number Pe^* optimiuzed by the cutting speed and kerf width versus absorbed dimensionless power.

The minimal achevable cut surface roughness at the optimal cutting parameters is different for the two laser types. The minimal value R_z is about 10 μm for the CO_2 laser and 25 μm for the fiber laser at the sheet thickness of 5 mm.

3.2. Fusion cutting

The cutting with an inert gas differ significantly from the oxygen-assisted laser cutting, because there is no exothermic oxidation reaction as an extra energy source, material destroy on the cut front and cut front propagation follow another mechanisms. That is why there is a need for special investigations to determine the energy balance and conditions of high quality cut at the laser cutting with an inert gas.

Square samples were cut-out from the sheets of stainless steel 12X18H10T (analog to steel AISI 321). Nitrogen pressure in the cutting head was 1.3…1.6 MPa. All measurements were carried out at the laser power of 2 kW. The thickness of the cut sheets was 3 and 5 mm. For these thicknesses, the surface roughness was studied in association with the cutting speed, and, for each speed value, the position of the focused beam waist was optimized in respect to the sheet surface by the minimal-roughness criterion for each laser.

For the thicknesses of 3 and 5 mm, the cut surface roughness was studied in detail. To do this, roughness R_a was measured along the line of 3 mm length oriented in parallel to the sheet surface. The roughness was measured in 26 sections, i.e., for example, at the sheet thickness of 3 mm, the measurement was performed with the gap of 120 μm. The measurements show that the character of roughness value distribution differs for the used lasers, however, both for the fiber and CO_2 laser, one observes the depth inhomogeneity of R_a (almost two times). Note roughness increase for the CO_2 laser in the bottom part of the cut. The presented results show that the comparison of the cut samples by the roughness criterion in individual points (by height) may lead to improper conclusions, and it is necessary to use the values R_a averaged over then whole plate thickness. Total values of such an averaged roughness obtained at the optimized position of the focus about the surface for each cutting speed value V, are shown in Fig.7 for 3 and 5 mm. Evident that the average roughness is higher at low speed; it decreases as the speed rises to a certain degree and then remains constant up to the maximal critical value of the speed; then the undercut takes place.

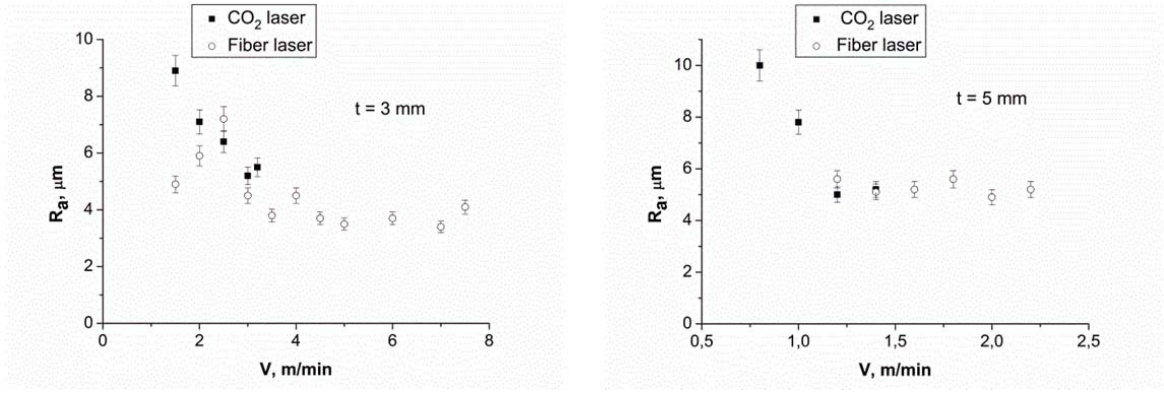

a b

Fig. 7. Roughness averaged by the sheet thickness versus cutting speed at W = 2 kW. (a) t = 3 mm; (b) 5 mm.

It is important to note that the values of the average roughness are close to each other at the optimal focus position and at the same speed for both lasers. The fiber laser however has the limit speed of about 1.5…2 times higher.

The dependence of the laser beam absorption coefficient on the cutting speed was measured during the cutting process by the same method as at the oxygen-assisted laser cutting. Fig. 8 presents the values of the laser beam absorption coefficient versus the cutting speed by the fiber and CO_2 lasers, for the thicknesses of 3 and 5 mm. Note significant excess of the A value for the CO_2 laser as compared to the fiber laser, the speed being the same.

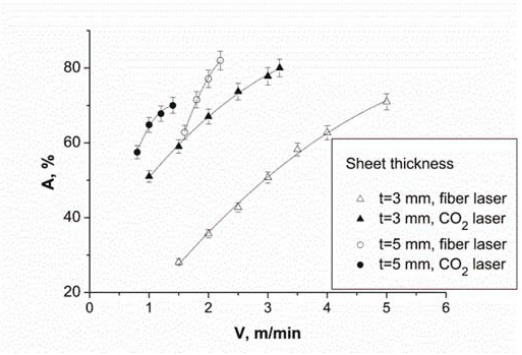

Fig. 8. Absorption coefficient A versus cutting speed.

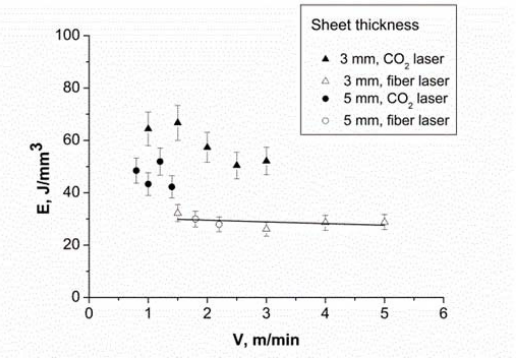

Fig. 9. Laser energy density in the unit of the removed material volume versus cutting speed.

Fig. 9 shows the dependence of the absorbed laser energy in the unit of the removed material volume on the cutting speed. The calculation involved the average cut width defined as the ratio of the transversal cross section area to the sheet thickness. Specific energy AW/Vtb slightly depends on the speed, its value is approximately the same for 3 and 5 mm and is 26…32 J/mm^3 for the fiber laser and (42…66) J/mm^3 for the CO_2 laser. The average value of the absorbed specific energy for the CO_2 laser is about 2 times higher.

To obtain more comprehensive and adequate physical picture of the process of laser cut formation, let us consider the energy balance of the cutting process when nitrogen is used as an assist gas. The balance equation is described with the known expression [4]:

$$AW = W_m + W_{cond} + W_{etc} \quad (1)$$

where A is the metal absorption coefficient, W is the laser power, W_m is the power consumed for metal heating and

melting, W_{cond} is the power lost from the cut area due to the thermal conductivity into the ambient material, W_{etc} is the other losses of the absorbed power including the convective and radiation cooling. The value W_m can be calculated from:

$$W_m = Vtb[\rho_m C_m(T_m - T_0) + \rho_m L_m + \rho_g C_g(T^* - T_m)] \quad (2)$$

where C_m, ρ_m and C_g, ρ_g are the process-average specific thermal capacity and density for the metal and melt, L_m is the latent heat, $T_m - T_0$ are the variations in the metal temperature during the cutting before the melting start, and $T^* - T_m$ is the variation of the melt temperature. In (2), the first term presents the power consumed for the metal heating up to the melting point, the second one – the same for the melting, and the third – for the heating up to T*.

In order to evaluate the heat losses, let us use the results of [10]:

$$W_{cond} = kt(T^* - T_0)3.2Pe^{0.868}, \quad (3)$$

Here, k is the material thermal conductivity. Substituting (2) and (3) in (1) and neglecting the other power losses [1], we have the general expression for the absorbed power density:

$$\frac{AW}{Vtb} = \rho_m L_m + \left[\rho_m C_m(T_m - T_0) + \rho_g C_g(T^* - T_m)\right] + \frac{1.6\rho_m C_m(T^* - T_0)}{Pe^{0.132}} \quad (4)$$

It should be noted that in [10], the channel half-width was used for the Peclet number calculation. In this work, the Peclet number is found from the full channel width, so, when using the expressions 3 and 4, the experimental Peclet values must be halved.

As is seen from (4), the density of the absorbed energy weakly depends on the Peclet number is governed by the only parameter T^*, i.e. the degree of melt overheating.

Fig. 10 shows that at the maximum speed of the CO_2 laser, the Peclet number values are close for both lasers. The absorbed power density, according to the data in Fig. 9, is much higher for the CO_2 laser than for the fiber laser.

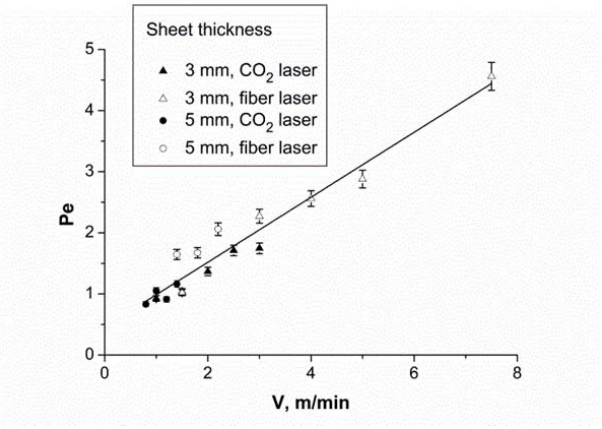

Fig. 10. Peclet number versus cutting speed.

It means, according to (4), that the melt must be overheated essentially, excessive energy must be present in it, but in the experiment the cut stopped in this case.

Thus, the obtained results contradict to each other – the cut stops as the melt is sufficiently overheated. The reason may be in the overestimated value of the laser power absorbed in the cut channel in the CO_2 laser case, hence the overestimated value of the specific volume energy input and melt temperature. The absorbed power was calculated as the difference between the power at the cut channel inlet and outlet according to a method [4, 9]. Possible beam reflection from the sheet surface, which is significant in the CO_2 laser case, is ignored here.

During the laser cutting, the channel forming and cut front propagation are cyclic. To start the cycle, the leading part of the beam must heat the surface section ahead of the cut front up to the melting point T_m. With the normal incidence, the absorption coefficient of the fiber-laser beam by stainless steel is much higher as compared to the CO_2 laser case. In [11], for $\lambda = 10.6$ мкм at the normal temperature, the given absorption coefficient is 2…5% , and this value rises up to 10% when the material is heated up to 1,000 ^{0}C, whereas for $\lambda = 1.07$ мкм, the absorption has the value of about 30% and weakly depends on the temperature. The body surface temperature being heated by a moving surface source of permanent intensity decreases as the source motion speed rises. At a certain speed, the conditions of the channel initiation disappear; the surface temperature is below the melting point. The surface temperature under the fiber-laser beam action decreases down to the melting point at the higher speed than it does in the CO_2 laser case, since in the fiber-laser case, the absorption coefficient is higher and the value of the absorbed laser power is higher, too. The conditions of the cut channel initiation disappear at the higher speed in the fiber-laser case; it may be the reason of the higher value of the maximal cutting speed when the laser power is the same as in the CO_2 laser case.

Another physical mechanism of the cut front propagation takes place in the oxygen-assisted laser cutting of the low-carbon steel. The process of the oxygen-assisted laser cutting can be described as the forced combustion of iron, and the front propagation occurs as cyclic combustion waves [9]. The cut front periodically separates from the leaser beam, and not the laser beam but the exothermic reaction of iron oxidation is the main initiator of the channel formation. Just insignificant part of the laser energy comes onto the sheet surface at the normal incidence and may be reflected. Moreover, metal surface oxidation during the oxygen-assisted laser cutting increases the absorption coefficient and reduces the reflected radiation proportion. Hence, the technique of the absorption coefficient measurement [4, 9] used in this work should give lesser errors in the oxygen-assisted laser cutting case.

4. Conclusion

The processes of low-carbon and stainless steel cutting by the fiber and CO_2 lasers were compared experimentally, providing that the cut surface roughness should be minimal. The laser power absorption coefficient was measured during the cutting, the absorbed laser energy E was found in respect of the material volume unit removed from the cut channel. During the oxygen-assisted laser cutting of low-carbon steel, the minimal cut-surface roughness is reached when E is equal to 11…13 J/mm^3, both for the fiber and CO_2 lasers. The minimal roughness is reached at the Peclet number 0.35…0.4 in the fiber-laser case, 0.45…0.55 in the CO_2-laser case.

In the fusion-cutting of stainless steel, the specific energy E is different when the cut surface roughness is minimal. The optimal speed corresponding to the minimal roughness coincides with the maximal speed. The lower value of this speed in the CO_2 case correlates with the higher value of the specific absorbed energy *E*.

This conflicting result may be caused by the technique of the laser-beam absorption coefficient in the cut channel when the absorbed power is measured is the difference between the power value at the channel inlet and outlet. This approach neglects the beam power part which strikes the sheet surface normally and might be reflected. This part of the beam must heat the metal up to the melting point and initiate the cut channel formation. Since the absorption coefficient for the fiber-laser beam is higher at the normal incidence than in the CO_2 case, the channel initiation conditions on the sheet surface disappear at higher speeds. Thus not the lack of energy, but the breach of conditions of the cut channel formation on the sheet surface may be the potential reason of the speed limitation, when the CO_2 laser cuts stainless steel with an inert gas.

References

Powell J, Kaplan AFH. A technical and commercial comparison of fiber laser and CO_2 laser cutting. In Proc. 31th International Congress on Applications of Lasers and Electro-Optics, Anaheim, CA, USA; 2012, p. 277-281.

Mahrle A, Beyer E. Theoretical aspects of fibre laser cutting, *J. Phys.D: Appl. Phys* 2009; 42:175507.

Petring D, Schneider F, Wolf N. Some answers to frequently asked questions and open issues of laser beam cutting. In Proc. 31th Congress on Applications of Lasers and Electro-Optics, Anaheim, CA, USA; 2012, p. 43-48.

Scintilla LD, Tricarico L, Wetzig A, Beyer E. Investigation on disk and CO_2 laser beam fusion cutting differences based on power balance equation, *Int. J. of Mach. Tools Manuf.* 2013; 69:30–37.

Hirano K, Fabbro R. Possible explanations for different surface quality in laser cutting with 1 and 10 μm beams. *J. Laser Applications* 2012; 24:012006.

A.G. Malikov, A.M. Orishich, V.B. Shulyatyev. Experimental optimization of the gas assisted laser cutting of thick steel sheets. *Quantum electronics* 2009; 39:547–551.

Malikov AG, Orishich AM, Shulyatyev VB. Scaling laws for the laser-oxygen cutting of thick-sheet mild steel. *Int. J. of Mach. Tools Manuf.* 2009; 49:1152–1154.

Afonin YuV, Golyshev AP, Ivanchenko AI, Malov AN, Orishich AM, Pechurin VA, Filev VF. Shulyat'ev VB. High-quality beam generation in a 8-kW CO_2 laser. *Quantaum Electron* 2004; 34:307–309.

Miyamoto I, Maruo H. Mechanism of laser cutting. *Welding in the world* 1991; 29:283–294.

Prusa JM, Venkitachalam G, Molian PA. Estimation of heat conduction losses in laser cutting. *Int. J. Mach. Tools Manuf.* 1999; 39:431–458.

Hugel H, Dausinger F. Fundamentals of laser-induced processes. In: Poprave R, Weber H, Herziger G, editors. *Laser Physics and Applications, Subvolume C: Laser Applications*, Berlin: Springer-Ferlag; 2004, p. 3–25